Artificial Organs

Theoretical Foundations of a Starling-Like Controller for Rotary Blood Pumps

*†Robert Francis Salamonsen, ¶¶Einly Lim, ***Nicholas Gaddum, ‡Abdul-Hakeem H. AlOmari, ¶**Shaun David Gregory, ¶††Michael Stevens, ††David Glen Mason, ‡‡John F. Fraser, ¶Daniel Timms, §§Mohan K. Karunanithi, and §Nigel Hamilton Lovell

**Department of Epidemiology and Preventive Medicine, Monash University; †Department of Intensive Care, Alfred Hospital, Melbourne, Victoria, Australia; ‡Biomedical Engineering Department, University of Dammam, Kingdom of Saudi Arabia; §Graduate School of Biomedical Engineering, University of New South Wales, Sydney, New South Wales; ¶ICET Laboratory, Critical Care Research Group, University of Queensland; **Institute of Health and Biomedical Innovation, Queensland University of Technology; ††School of Information Technology and Electrical Engineering, University of Queensland; ‡‡Critical Care Research Group, Intensive Care Unit, The Prince Charles Hospital, and University of Queensland; §§Australian eHealth Research Centre, CSIRO, Brisbane, Queensland, Australia; ¶¶Department of Biomedical Engineering, University of Malaysia, Kuala Lumpur, Malaysia; and ***Department of Imaging Sciences, King's College London, London, UK*

Abstract: A clinically intuitive physiologic controller is desired to improve the interaction between implantable rotary blood pumps and the cardiovascular system. This controller should restore the Starling mechanism of the heart, thus preventing overpumping and underpumping scenarios plaguing their implementation. A linear Starling-like controller for pump flow which emulated the response of the natural left ventricle (LV) to changes in preload was then derived using pump flow pulsatility as the feedback variable. The controller could also adapt the control line gradient to accommodate longer-term changes in cardiovascular parameters, most importantly LV contractility which caused flow pulsatility to move outside predefined limits. To justify the choice of flow pulsatility, four different pulsatility measures (pump flow, speed, current, and pump head pressure) were investigated as possible surrogates for LV stroke work. Simulations using a validated numerical model were used to examine the relationships between LV stroke work and these measures. All were approximately linear (r^2 (mean ± SD) = 0.989 ± 0.013, $n = 30$) between the limits of ventricular suction and opening of the aortic valve. After aortic valve opening, the four measures differed greatly in sensitivity to further increases in LV stroke work. Pump flow pulsatility showed more correspondence with changes in LV stroke work before and after opening of the aortic valve and was least affected by changes in the LV and right ventricular (RV) contractility, blood volume, peripheral vascular resistance, and heart rate. The system (flow pulsatility) response to primary changes in pump flow was then demonstrated to be appropriate for stable control of the circulation. As medical practitioners have an instinctive understanding of the Starling curve, which is central to the synchronization of LV and RV outputs, the intuitiveness of the proposed Starling-like controller will promote acceptance and enable rational integration into patterns of hemodynamic management. **Key Words:** Left ventricular assist device—Implantable rotary blood pump—Heart failure—Physiological control—Starling mechanism.

Although implantable rotary blood pumps (IRBPs) have conferred many benefits, control of pump flow by adjustment of pump speed is challenging. A physiological controller for pump flow would therefore be a significant advance. Recent developments of so-called physiological controllers of IRBPs have been adequately reviewed (1–4). With the possible exception of the Berlin Heart Incor (Berlin Heart, Berlin, Germany) (4), none have gained clinical acceptance in commercial devices. Details of these methods are typically foreign to

doi:10.1111/j.1525-1594.2012.01457.x

Received December 2011; revised January 2012.

Address correspondence and reprint requests to Professor Robert F. Salamonsen, C/O ICU Office, Alfred Hospital, Prahran, Vic. 3181, Australia. E-mail: r.salamonsen@alfred.org.au; rsalamon@iinet.net.au

TABLE 1. *Summary of pulsatility measures by brand and manufacturer*

Brand of IRBP	Manufacturer	Pulsatility measure
Incor (4)	Berlin Heart, Berlin, FRG	ΔP_{IRBP}*
Heartmate II (15)	Thoratec Corporation, CA, USA	Flow†‡§
Heartmate III (16)	Thoratec Corporation, CA, USA	Flow†‡§
Heartware (17)	HeartWare, Inc., MA, USA	Flow†‡§¶
Duraheart (18)	Terumo Heart, Inc., MI, USA	Flow†‡§¶
Levacor (15)	World Heart, UT, USA	Flow†‡§
MicroMed Heart Assist (19)	MicroMed Cardiovascular, Inc., TX, USA	Flow**
VentrAssist (14)	Ventracor, NSW, Australia	Speed††
Coraide (20)	Cleveland Clinic, OH, USA	Flow†‡§

ΔP, differential pressure.
*Derived from lateral force on magnetic bearing.
†Derived from current.
‡Derived from rotor speed.
§Derived from pump voltage.
¶Derived from hematocrit.
**Measured with ultrasonic flow probe on outlet cannula.
††Intrinsic pump parameter.

medical thinking and most clinicians do not understand the details of how the controller works. Consequently, if inappropriate patient responses occur, clinicians will lose confidence in the controller and usually will revert to manual speed control. This however is unphysiologic, as it decouples the pump from the cardiovascular system. This occurs because the IRBP lacks a feature like the Starling mechanism which synchronizes left ventricular (LV) and right ventricular (RV) outputs irrespective of variations in venous return (5). This decoupling can have deleterious effects when cardiovascular states change. Most common is ventricular suction which may cause endocardial damage, septal shift, mitral incompetence, and ventricular arrhythmias (6,7). Pulmonary edema less commonly occurs if the combined outputs of LV and pump flow are sufficiently below RV output.

Medical practitioners however are familiar with Starling's law of the heart and understand how it synchronizes outputs of both ventricles (8). If the pump had a Starling-like response to changes in LV preload, the combined output of the LV and IRBP would synchronize with the RV output across varying physiological states, thus eliminating overpumping and underpumping. A Starling-like controller ideally would use an implantable pressure transducer to continuously monitor LV end-diastolic pressure (9). Although a number of these transducers are under development (10–13), none have gained clinical acceptance in commercial devices.

In previous work (14), we have demonstrated that when the aortic valve is not opening, speed pulsatility of the VentrAssist LVAS (Ventracor) is related to left ventricular stroke work (LVSW) by a shallow curve which can be fitted to a second-order polynomial equation (coefficient for squared term ≤ 0.04) and which can be approximated as linear with clinically acceptable precision. Consequently, this and other pulsatility measures induced by the contracting LV may act as noninvasive surrogates for LVSW. The measures listed in Table 1 (4,14–20) are features of commercial IRBPs. However, there has been no formal study of which is best in a variety of clinical states.

In this study, a Starling-like pulsatility controller based on the flow pulsatility was derived. The choice of flow pulsatility was then justified by examining the performance of four different pulsatility measures to determine which best indicated LVSW at different levels of LV contractility (LVC). Finally, the functional principles of the Starling-like controller were then validated over a range of cardiovascular states.

METHODS

Basic methods

A previously described and validated (1,21) computer model of the cardiovascular system and IRBP (VentrAssist LVAS) was used to study relationships between LVSW and the pulsatility measures reviewed in Table 1. The animal model was quantified with data obtained from the literature and from in vivo pig data and was implemented in Matlab (The MathWorks, Inc., Natick, MA, USA).

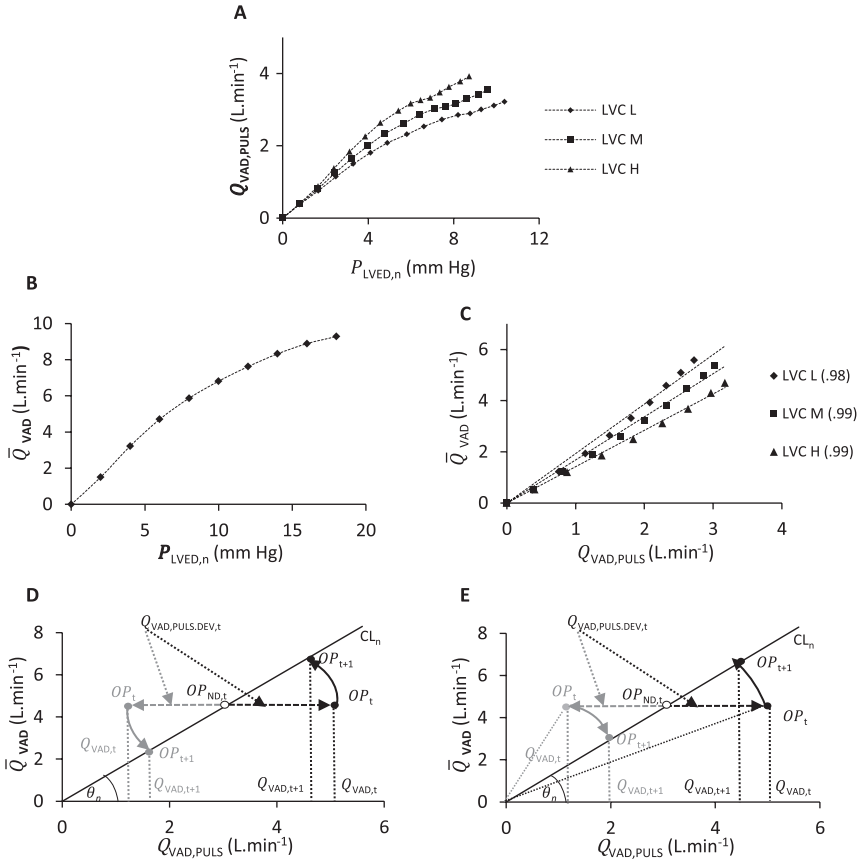

FIG 1. Derivation of the pump control line and action by controller. (A) Pump flow pulsatility ($Q_{VAD,PULS}$) versus normalized left ventricular end-diastolic pressure ($P_{LVED,n}$) across three different values for left ventricular contractility (LVC). Low (L), medium (M), high (H). (B) Starling-like characteristic imposed by controller on average pump flow ($\bar{Q}_{VAD}$) in proportion to normalized left ventricular end-diastolic pressure ($P_{LVED,n}$). (C) Relationship between average pump flow ($\bar{Q}_{VAD}$) and pump flow pulsatility ($Q_{VAD,PULS}$) obtained by substituting $Q_{VAD,PULS}$ for $P_{LV,ED,n}$ in B using relationship defined in A. (D and E) Performance of first and second methods to correct for the deviation in flow pulsatility occurring in the time interval, t. ($Q_{VAD,PULS,DEV,t}$) so that the new operating point, OP_{t+1} is returned along radial pages with different origins path back to the control line. The suffix ND indicates "not deviated." Items in gray indicate response following negative deviations in $Q_{VAD,PULS,DEV,t}$ and items in black indicate responses to positive deviations.

Four pulsatility measures (flow, speed, current, and differential pressure across the IRBP) were extracted from peak-to-trough amplitude of fluctuations over the cardiac cycle induced by the contracting LV. In all simulations, pump speed was reduced from 2400 rpm in steps of 50 rpm to 1800 rpm to progressively increase LV filling and thereby LVSW. This range covered states where the aortic valve was both open and closed. LVSW was calculated using the pressure volume loop area method using Eq. 1:

$$SW_{LV,PVLOOP} = \int_o^V P_{LV} \cdot dV \qquad (1)$$

where V represents the stroke volume (SV) of the heart, and P_{LV} refers to pressure of the LV. Units for volume were mL, flow, mL/s; a value of 1.3331×10^{-4} was used to convert LVSW from mm Hg/mL to joules. Linear regressions were calculated using Excel 2010 (Microsoft Corporation, Redmond, WA, USA). All simulation results were initially screened for suction beats which were easily recognized in each simulation by spurious increases in ventricular assist device (VAD) flow pulsatility at the highest pump speeds. All suction beats were deleted before detailed analysis.

Derivation and evaluation of the "Starling-like" pulsatility controller

Derivation of the pump control line

An initial simulation was conducted to evaluate the response of flow pulsatility ($Q_{VAD,PULS}$) to changes in normalized LV end-diastolic pressure ($P_{LVED,n}$) across three different values for LVC (Fig. 1A). These relationships allow substitution of $Q_{VAD,PULS}$ for $P_{LVED,n}$ in the control characteristic for the IRPB which was adapted from that proposed by Guyton for the natural LV (22) (Fig. 1B). When this substitution is made (Fig. 1C), the resultant control lines are seen to be linear over a range of values for LVC ($r^2 \geq 0.98$). These control lines are thus equivalent to the Frank–Starling curve when expressed in terms of pulsatility rather than $P_{LVED,n}$. The gradients of the control lines are analogues of different amplitudes for the Starling curve and are defined by the angles (θ) they make with the "x" axis. When flow pulsatility is used, the gradients of the control lines are dimensionless ratios called here pump assist ratios.

Starling-like control is applied by an iterative method. In this application, the magnitude of the time step is sufficient for eight heartbeats, that is,

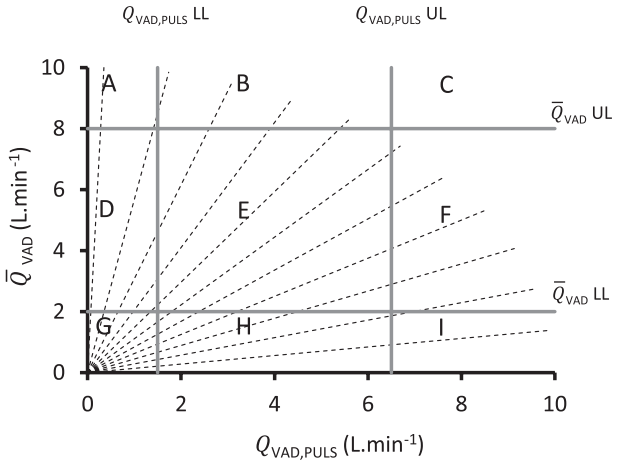

FIG 2. Making the controller adaptive. (A) Typical set of control lines of differing slopes where the slope indicates the pump assist ratio. (B) Imposed upper (UL) and lower limits (LL) on average pump flow ($\bar{Q}_{VAD}$) and flow pulsatility ($Q_{VAD,PULS}$). The graph area is separated into nine zones (A–I) which have different implications for the Starling-like controller.

10 s or less depending on the heart rate. At the end of any time step (t), after measurement or estimation of $\bar{Q}_{VAD,t}$ and $Q_{VAD,PULS,t}$ (23,24), these values define the deviation of the operating point (OP_t) from the control line as the cardiovascular state changes. To implement Starling-like control, at the end of each time step, a new value for $\bar{Q}_{VAD,t+1}$ must be derived which is designed to return $Q_{VAD,PULS,t}$ to the control line. The magnitude and direction of the change in $\bar{Q}_{VAD,t}$ depends on the magnitude and direction (postive or negative) of the deviation in $\bar{Q}_{VAD,PULS,t}$. Although there are a number of possible strategies to do this, the two considered to be most appropriate are presented here mathematically as Eqs. 2 and 3. These calculate target values of average pump flow for the next time step ($\bar{Q}_{VAD,t+!}$) that will return the new operating point (OP_{t+1}) along different paths back to the control line of gradient specified by the angle θ.

$$\bar{Q}_{VAD,t+!} = \bar{Q}_{VAD,t}(1-\cos\theta^{-1}) + Q_{VAD,PULS,t}\sin\theta \quad (2)$$

$$\bar{Q}_{VAD,t+1} = \left(\sqrt{(\bar{Q}_{VAD,t})^2 + (Q_{VAD,PULS,t})^2}\right)\sin\theta_n \quad (3)$$

These paths are graphed in Fig. 1D,E.

Making the controller adaptive

To make the controller adaptive, 11 control lines of gradients, each differing by eight degrees, were developed to assist the LV by differing amounts in response to sustained changes in LVC (Fig. 2). The method used to move the operating point from any control line to another line ensures that the interval between the operating points and the origin of the "x" and "y" axes on the two lines remain the same. The equation used to calculate the average pump flow ($\bar{Q}_{VAD,n+!}$) appropriate for the operating point (OP_{n+1}) on the new control line (n + 1) is given in Eq. 4:

$$\bar{Q}_{VAD,n+!} = \bar{Q}_{VAD,n}\sin\theta_{n-1}\sin\theta_{n+1} \quad (4)$$

Full derivations of Eqs. 2–4 are available from the corresponding author on request.

Finally, rules are developed to determine which control line is used at any one time. Upper and lower limits for average pump flow and flow pulsatility (Fig. 2) are imposed to define a zone of acceptability (labeled as E in Fig. 2) for the operating point within which no change in gradient is indicated. If the operating point migrates to zones F, H, or I, an increase in gradient is required. Similarly, if the operating point enters A, B, or D, a fall in gradient is indicated. In the unlikely event of the operating point moving to zones C or G, then a change in gradient will not fix the problem. In this case, the controller should revert to a default value for pump speed and an alarm sounded so that a change in medical treatment can be implemented. The use of multiple control lines introduces the issue of which line to choose at the commencement of Starling-like control. This is achieved simply by choosing the control line to which current values of average pump flow and flow pulsatility are closest when the patient has achieved an optimum circulatory state as defined by the medical practitioner based on clinical experience and results of investigations like echocardiography.

Justification for use of flow pulsatility in the Starling-like controller

Simulations were conducted to evaluate the four pulsatility measures. The first, conducted at four values for LVC, determined which measure responded most appropriately to changes in LVSW. The second determined how variations in each of the five cardiovascular states (LVC and RV contractility, blood volume, systemic vascular resistance, and heart rate) affected the relationship between LVSW and pump flow pulsatility, the measure of choice. The range of states tested is given in Table 2. A change in gradient of the relationship between pulsatility measures and LVSW invariably occurred when the aortic valve opened. Gradients before this occurred were expressed by the angle the response line made with the abscissa in degrees ($\theta_{Original(deg)}$), while deviations

TABLE 2. *Range of different cardiovascular states used in model simulations*

CVS parameter		Low	Medium	High	Very high
LV contractility (E_{max})	(mm Hg/mL)	1.0	1.5	2.0	3.0
RV contractility (E_{max})	(mm Hg/mL)	0.3	0.45	0.6	0.9
Systemic vascular resistance	(mm Hg/L/min)	8.66	13.6	18.6	23.6
Blood volume	(L)	4.5	4.75	5.25	5.5
Heart rate	(min^{-1})	50	70	90	130

The model was populated with parameter values appropriate for a porcine model (approximation to human subject) identified in previous work (1,21); the step changes in values of parameters changing from high to very high are larger than the previous steps to ensure that a wide range of cardiovascular states are studied.

from linearity were assessed by the angle between the two regression lines $\theta_{Deviation(deg)}$ fitted to gradients before and after the opening of the aortic valve. To quantify these deviations from linearity, the change from the initial slope in percent (*Deviation*(%)) was calculated using Eq. 5. The origin for calculation of θ was the point of intersection of linear regression lines for relationships before and after the opening of the aortic valve.

$$Deviation(\%) = \frac{\theta_{Deviation(deg)}}{\theta_{Original(deg)}} \times 100 \qquad (5)$$

Assessment of the control strategy

The control strategy was assessed by a series of simulations in which the system (pump flow pulsatility) response to primary changes in pump flow was evaluated across differences in each of the five cardiovascular states. The appropriateness or otherwise of the criteria for moving to lines of different gradient could then be evaluated.

RESULTS

Justification for use of flow pulsatility as the measure of choice

Figure 3 illustrates four different pulsatility measures and the way each responded to increases changes in LVSW across three different values for LVC. These demonstrated a linear relationship between pump flow pulsatility and LVSW until the aortic valve began to open. Beyond this point, a deviation from linearity which invariably occurred is explained by preferential ejection of blood through the low-resistance pathway of the open aortic valve. The magnitude of this deviation was least (60%) for pump flow pulsatility, compared to the other measures which were 78% for pressure head across the

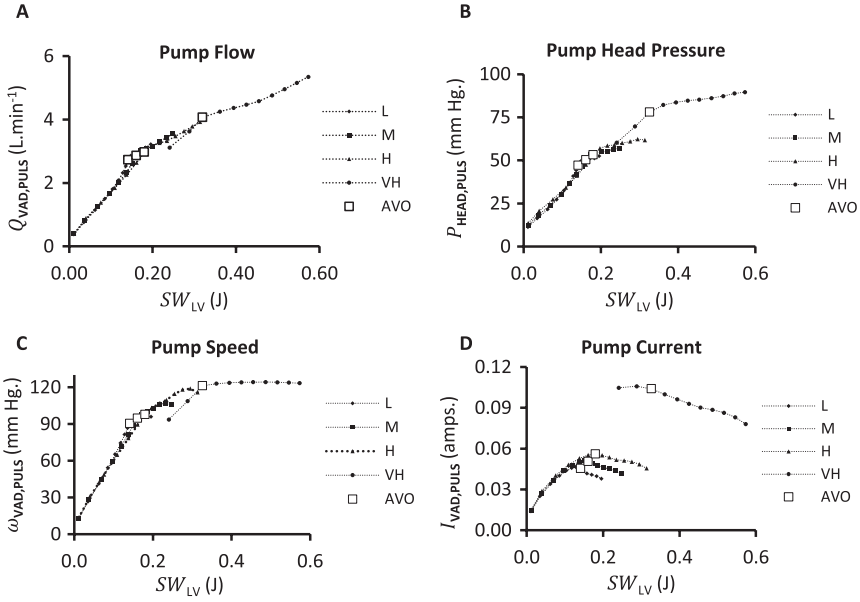

FIG 3. Performance of different pulsatility indices as indicators of LV stroke work across changes in LV contractility. Pulsatility measures: $Q_{VAD,PULS}$, flow; $P_{HEAD,PULS}$, head pressure across pump; $\omega_{VAD,PULS}$, speed; $i_{VAD,PULS}$ current; SW_{LV} (J), stroke work of LV; L, low; M, medium; H, high; VH, very high LV contractility; AVO, aortic valve opens.

pump, 100% for speed pulsatility, and 142% for current pulsatility. This confirmed the appropriateness of pump flow pulsatility as the measure of choice.

Changes in each of the five cardiovascular states indicated a surprisingly uniform linear relationship between pump flow pulsatility and LVSW while the aortic valve was closed. Slopes of regression lines for flow pulsatility on LVSW, expressed as degrees for the angle each made with the abscissa, varied from 43 to 52° across differences in all the five cardiovascular states. After the aortic valve opened, all relationships displayed a relatively uniform deviation from linearity, which lay within limits of 53–62%. However, the LVSW at which the aortic valve opened varied considerably across changes in the five cardiovascular states. Lower and upper limits varied between 0.08 and 0.16 J and 0.24 and 0.34 J, respectively.

Assessment of the Starling-like controller

Figure 4 indicates the response of pump flow pulsatility to primary variations in pump flow across differences in all five cardiovascular states. The axes have been reversed in this simulation to accommodate the status of pump flow as the independent variable. Hence, the control line of the lowest gradient in this context defined the maximum assist ratio. Changes occur both in the slope of the response and the point at which the aortic valve opens. The operating points appropriate for different control lines are seen at the points of intersection of the control and response lines. Figure 4 also shows that migration to a higher pump assist ratio moves operating points downward and to the right, while migration to a lower assist ratio achieves the opposite. The set of control lines is also seen to be sufficient to accommodate large changes in responses of average pump flow to changes in flow pulsatility across a wide range of clinical states. Figure 4 shows settings for upper and lower limits for both flow and flow pulsatility which are medically appropriate for changes in most states, but not all. For example, the upper limit for pump flow as set for Fig. 4 is ideal for changes in LVC and RV contractility and systemic vascular resistance but not for changes in blood volume and heart rate.

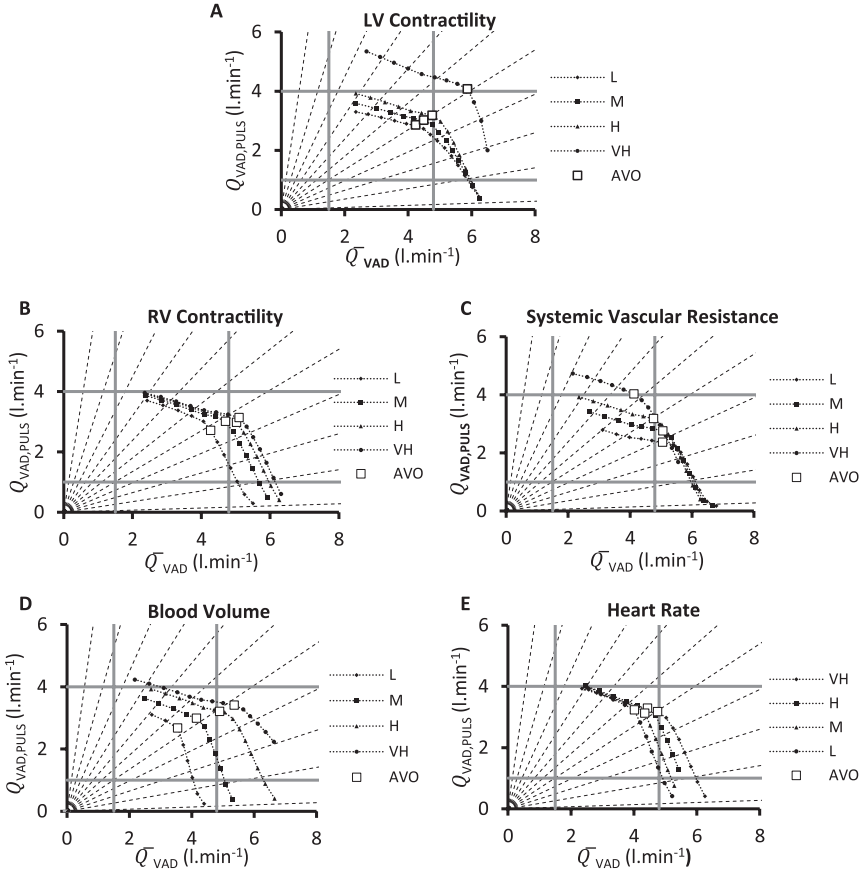

FIG 4. System (flow pulsatility) response to primary changes in pump flow. Axes have been reversed as pump flow in this simulation was the independent variable. Added vertical lines, lower and upper limits for flow pulsatility; Horizontal lines, lower and upper limits for average pump flow. Dotted lines indicate set of control lines where, in contrast to Figs. 1 and 2, the line of lowest gradient indicates the highest pump assist ratio. L, low; M, medium; H, high; VH, very high refer to the magnitude of parameters quantifying each state as detailed in Table 2; AVO, aortic valve opens; $Q_{VAD,PULS}$, LVAD flow pulsatility; Q_{VAD}, average VAD flow.

DISCUSSION

A central finding of this study is the linear relationship between pump flow pulsatility and LVSW as long as the aortic valve is closed. The main achievement of this study is the rigorous derivation of a Starling-like controller in which average pump flow varies with pump flow pulsatility along a control line of predefined gradient. The controller has the ability to synchronize the combined left-sided output (LV plus IRBP) with that of the RV, thus achieving true physiological control of the circulation. Furthermore, the controller can migrate to control lines of different gradients if the operating point moves outside predefined limits. Use of a set of control lines of different gradients allows stabilization of LVSW across a range of different flow pulsatilities and by inference ventricular volumes ranging from zero pulsatility at minimum volume (full pump assist) to the point at which the aortic valve opens (partial assist). Beyond this point, there is a reduction in the sensitivity at which flow pulsatility responds to increasing LVSW which may be appropriate for conditioning the recovering ventricle, but not for support of a failing heart. In order to maintain the operating point on the controller line, closed loop control of pump flow via adjustment of pump speed must be incorporated. This requires the implementation of a feedback control system that adjusts pump speed to minimize the error between the target pump flow and measured or estimated pump flow. An example of such a feedback control mechanism is proportional plus integral plus derivative control, as used by Stevens et al. (25), and PI control, as reported by Moscato et al. (3). An important physiological requirement for the controller is that it is very fast, that is, that the target pump flow is substantially attained within eight heartbeats (approximately 10 s or less). Otherwise, ventricular suction cannot be prevented, particularly if the Starling-like controller is operating on control lines of low gradient. At this stage, we are not sure which of the two proposed methods for returning the operating point to the control line will prove to be the most rapid and stable from a control point of view. The essential difference between the two methods is that the second one, using a circular path with an axis of rotation at the origin of the "x" and "y" axes, is gentler particularly with control lines of high gradient. Potentially faster control modes including sliding mode and model predictive control are also under examination in our research group.

Although many claim a physiological character for their control methods, usually on the basis of some preload sensitivity (1–4), this does not satisfy the requirements for a Starling-like controller. Preload sensitivity must be comparable to that of the LV (8). It should also be maximal at very low LV preloads (to avoid ventricular suction), but fall continuously in a nonlinear fashion as LV preload increases to become negligible at very high preloads to minimize overpumping. The third major requirement is that the amplitude of the Starling curve can be increased or decreased as a whole to allow the heart to compensate for changing metabolic requirements as in exercise or emotional stress (26). Two approaches to physiological control which come close to Starling-like control deserve specific mention. Arndt et al. (4) describe a method for the INCOR device which is preload sensitive to a degree presumably on the basis of its known relationship between head pressure and pump flow at a single speed setting but has two operating points selectable by the attending physician. The first controls ventricular volume at a level close to, but safely separated from the point of zero pulsatility (full assist), while the second controls ventricular volumes at the point where the aortic valve begins to open (partial assist). We believe the deficiency with this system is that other operating points between these two extremes are not utilized. Consequently, the controller does not have fine control of LVSW and the ability to adjust support for small differences in LVC. Moscato et al. (3) propose a control method, which stabilizes the load on the LV (outflow impedance) irrespective of the body's blood flow requirements and presumably LV preload. Furthermore, the level of outflow impedance for the LV is preset depending on LVC. For example, if the LV is very weak, the pump increases average flow to decrease the LV's outflow impedance, whereas if the LV is stronger, the contribution from the pump can be reduced. However, it does require estimation or measurement of LV pressure as well as pump flow. Also, because the controller works to a set point for LV afterload, it requires the pump controller to completely compensate for variations in the body's blood flow requirements. In contrast, our system allows the LV to share variations in load to a variable extent depending on the gradient of the pump control line used. The latter confers the benefit of intermittent opening of the aortic valve and exposing the heart to controllable variations in load. It is also presumably less taxing for the controller.

Limitations of pulsatility-based control

There are many other requirements for efficient pulsatility control. There must be sufficient residual LVC to produce a useable pulsatility signal. As the aortic valve begins to open at lower pulsatilities as

LVC decreases, a higher gradient is required for the control line which reduces the precision of control. The situation may be improved somewhat by adjusting pump geometry and feedback speed controller to maximize the flow pulsatility through the IRBP (27).

However, in the limiting case, where the LV has no remaining contractile reserve, pulsatility control is not feasible, and the only solution is a pump such as the Thoratec P-VAD which cannot generate the large levels of suction typical of an IRBP.

RV function is also important. While the RV must have sufficient contractility to return the systemic venous return to the LV, it must not be too dominant. If it is, increasing average pump flow will not achieve the shift in fluid volume between the pulmonary and systemic circulations necessary to reduce LV preload (8). This is because the normal RV almost completely accommodates for the increased left-sided flow induced by increasing pump flow because it is very sensitive to small increases in preload (28). Consequently, there is a real risk of inducing unwanted excesses in LV output.

The marked variations in aortic valve opening across different circulatory states provide an additional challenge as the controller loses sensitivity once the aortic valve begins to open. It is therefore important to set the upper limit for pump flow pulsatility at an appropriate level and to reset it as required. In addition, irregular cardiac rhythms, particularly atrial fibrillation, will cause irregular SVs and any pulsatility mode to be unstable (29). Hence, an averaging filter for flow pulsatility index needs to be employed. Finally, if the controller does not implement corrections in average pump flow quickly enough, ventricular suction could occur. Because the relationship between pump flow and flow pulsatility is not monotonic (4), the apparent increase in pulsatility caused by suction induces a spurious increase in VAD flow which aggravates the suction condition. Therefore, an effective suction detector (30,31) is mandatory.

One of the limitations of using flow pulsatility as a surrogate for LVSW is that in contrast to preload, the same changes in pulsatility can be caused by a reduction in LV filling or contractility. This is a problem because medical management of the two is very different. However, changes in preload are often transient, for example, reductions due to coughing, defecation, change of posture, or quickly alleviated by fluid input, whereas in most circumstances, a change in LVC is likely to be long lasting once inotropes are weaned and the patient has progressed through the early postoperative period. Therefore, in the implementation of the Starling-like pulsatility controller, suitable delays need to be incorporated before the controller migrates to a control line of different gradient. Similarly, the sounding of the alarm should not be implemented with the first migration into the unsolvable areas but should also be somewhat delayed.

Clinical experience indicates that if the IRBP inlet cannula becomes partially obstructed in systole by mobile ventricular tissue adjacent to its orifice, this can mask the normal relationship between average pump flow and flow pulsatility. In these cases, pulsatility-based strategies to control average pump flow will not work. Dynamic obstruction of the inlet orifice by mobile tissue during systole should be excluded via echocardiography before the implementation of pulsatility control.

Deficiencies of the current study

The control characteristic for pump flow is not modeled on the original concept developed by Starling (5) in which LVSW is directly dependent on LV preload but Guyton's subsequent modification (22) in which it is LV output that is dependent on LV preload. However, a rigorous derivation would have required the pump to be calibrated in terms of work per heartbeat which is not feasible without continuous monitoring of the pressure gradient across the pump in addition to flow. Our defense is that although the two curves are very different at high preloads, they have a similar shape for preloads below 15 mm Hg which should be the maximum encountered in any well-assisted LV. The present model does not include uncertainties based on errors in measurement or estimation of pulsatility measures and pump flow. This may have implications for methods of noninvasive estimation of average pump flow and flow pulsatility where the estimation error might be highly significant (15). Finally, we have yet to publish validation studies of mathematical model and controller in a mock circulatory loop.

The philosophy of this method is for the attending medical practitioners not only to understand how the controller works but, with the aid of their experience and tools like echocardiography, to undertake joint management of both controller and patient. While upper and lower limits have been proposed to ensure safety under all circumstances, we imagine that most of the time a stable patient will operate on a single control line which can be set by the attending physician and reset as necessary to accommodate for long-term changes in LVC. The obligatory involvement of physicians in the fine-tuning of the control policy may be seen as a disadvantage. However, we would argue that if physicians understand the way the controller

works, and are intimately involved with its adjustment, this will facilitate their acceptance of the technique. This applies particularly in clinical situations where inappropriate patient responses seem to be occurring. Insight into the controller's mechanism and the ability to fine-tune its performance should give the clinician the confidence to continue with the control strategy in combination with other adjustments to fluid and drug management. This is a critical consideration for all control strategies. Attending physicians do however have to relinquish their current preoccupation with control of pump flow and focus on control of the work output of the LV, leaving autoregulation of flow in the tissues and the nonfailing RV to control cardiac output (22,28).

Future work

The first priority is to complete validation studies of model and controller in a mock circulatory loop.

Other projects include use of body sensors such as accelerometers to control migration, to control lines of higher gradients (2), to compensate for the failure of pump flow pulsatility, to increase adequately, or even to decrease during physical exercise—thus overcoming the limitations of pulsatility to reflect the increased metabolic load involved. In addition, the noninvasive detection of aortic valve opening from analysis of pump waveforms (32), if sufficiently reliable, could be substituted for the manually imposed upper limit for flow pulsatility. In this way, variations in the point at which aortic valve opens in different hemodynamic states can be accommodated automatically. Finally, the recent publication of a study by AlOmari et al. (33) will enable us to develop a true Starling-like controller based on mean LV diastolic pressure.

CONCLUSION

This study, using numerical simulation techniques, establishes that pulsatility measures derived for IRBPs may be used as surrogates for LVSW. In addition, using the linearity of this relationship which persists while the aortic valve remains closed, a linear Starling-like control of average pump flow can be developed based on pump flow pulsatility rather than LV preload. This controller is able to vary its sensitivity to changes in flow pulsatility to adapt to long-term variations in LVC. To do this, it uses a set of control lines of progressively increasing gradients which emulate the varying amplitudes of the real Starling curve. Upper and lower limits for average pump flow and flow pulsatility form the basis for empirical rules controlling migration of the controller to different control line gradients. These limits are set and reset as required by attending physicians who will be able to integrate its settings into their strategies for total hemodynamic management.

Acknowledgments: This work was supported in part by an Australian Research Council Linkage grant with BiVACOR Pty. Ltd.

REFERENCES

1. Lim E, Dokos S, Cloherty SL, et al. Parameter optimized model of cardiovascular–rotary blood pump interactions. *IEEE Trans Biomed Eng* 2010;57:254–66.
2. Karantonis DM, Lim E, Mason DG, Salamonsen RF, Ayre PJ, Lovell NH. Non-invasive activity-based control of an implantable rotary blood pump: a comparative software simulation study. *Artif Organs* 2010;34:E34–45.
3. Moscato F, Arabia M, Colacino FM, Naiyanetr P, Danieli GA, Schima H. Left ventricle afterload impedance control by an axial flow ventricular assist device: a potential tool for ventricular recovery. *Artif Organs* 2010;34:736–44.
4. Arndt A, Nusser P, Lampe B. Fully autonomous preload-sensitive control of implantable rotary blood pumps. *Artif Organs* 2010;34:726–35.
5. Starling EH, Visscher MB. The regulation of the energy output of the heart. *J Physiol* 1927;62:243–61.
6. Volkron M, Voitl P, Ta J, Wieselthaler G, Schima H. Suction events during left ventricular support and ventricular arrhythmias. *J Heart Lung Transplant* 2007;26:819–25.
7. Reesink K, Dekker A, Van der Nagel T, et al. Suction due to left ventricular assist device control and management. *Artif Organs* 2007;31:542–9.
8. Salamonsen RF, Mason DG, Ayre PJ. Response of rotary blood pumps to changes in preload and afterload at a fixed speed setting is unphysiological when compared with the natural heart. *Artif Organs* 2011;35:E47–53.
9. Bullister E, Reich S, Sluetz J. Physiologic control algorithms for rotary blood pumps using pressure sensor input. *Artif Organs* 2002;26:931–8.
10. Bullister E, Reich S, d'Entremont P, Silverman N, Sluetz J. A blood pressure sensor for long-term implantation. *Artif Organs* 2001;25:376–9.
11. Fritz BJ, Cysyk J, Newswanger R, Weiss W, Rosenberg G. Development of an inlet pressure sensor for control in a left ventricular assist device. *ASAIO J* 2010;56:180–5.
12. Chow EY, Chlebowski AL, Chakraborty S, Chappel WJ, Irazoqui PP. Fully wireless implantable cardiovascular pressure monitor integrated with a medical stent. *IEEE Trans Biomed Eng* 2010;57:1487–96.
13. Ritzema J, Melton IC, Richards AM, et al. Direct left atrial pressure monitoring in ambulatory heart failure patients: initial experience with a new permanent implantable device. *Circulation* 2007;116:2952–9.
14. Salamonsen RF, Lim E, Mason D. Applied physiology of rotary blood pumps: how robust is the relationship between left ventricular stroke work and speed pulsatility of the VentrAssist rotary blood pump? *Artif Organs* 2009;33:A82.
15. Slaughter MS, Bartoli CR, Sobieski MA, et al. Intraoperative evaluation of the Heartmate II flow estimator. *J Heart Lung Transplant* 2009;28:39–43.
16. Farrar DJ, Bourque K, Dague CP, Cotter J, Poirier VL. Design features, developmental status and experimental results with the Heartmate III centrifugal pump. *ASAIO J* 2007;53:310–5.
17. LaRose JA, Tamez D, Ashenuga M, Reyes C. Design concepts and principle of operation of the HeartWare ventricular assist system. *ASAIO J* 2010;56:285–9.

18. Morshuis M, Schoenbrodt M, Nojiri C, et al. Durheart magnetically levitated centrifugal left ventricular assist system for advanced heart failure patients. *Expert Rev Med Devices* 2010;7:173–83.
19. Wieselthaler GM, Schima H, Hiesmayr M, et al. First clinical experience with the DeBakey VAD continuous-axial-flow pump for bridge to transplantation. *Circulation* 2000;101: 356–9.
20. Ochiai Y, Golding LAR, Massiello AL, et al. In vivo haemodynamic performance of the Cleveland Clinic CorAide blood pump in calves. *Ann Thorac Surg* 2001;72:747–52.
21. Lim E, Dokos F, Salamonsen RF, Rosenfeldt FL, Ayre PJ, Lovell NH. Numerical optimization studies of cardiovascular-rotary blood pump interaction. *Artif Organs* 2012;36:E110–E24.
22. Guyton A. *Circulatory Physiology: Cardiac Output and Its Regulation*. Philadelphia and London: W.B. Saunders Company, 1963;237–9.
23. AlOmari AH, Savkin AV, Karantonis DM, Lim E, Lovell NH. Non-invasive estimation of pulsatile flow and differential pressure in an implantable rotary blood pump for heart failure patients. *Physiol Meas* 2009;30:371–86.
24. Zhang XT, AlOmari AH, Savkin AV, et al. In vivo validation of pulsatile flow and differential pressure estimation models in a left ventricular assist device. *Conf Proc IEEE Eng Med Biol Soc* 2010;2010:2517–20.
25. Stevens MC, Gaddum NR, Piercy MJ, et al. Frank–Starling control of a left ventricular assist device. *Conf Proc IEEE Eng Med Biol Soc* 2011;2011:1335–8.
26. Sarnoff SJ, Brockman SK, Gilmore JP, Linden RJ, Mitchell JH. Regulation of ventricular contraction. Influence of cardiac sympathetic and vagal nerve stimulation. *Circ Res* 1960;8: 1108–22.
27. Gaddum N, Fraser J, Timms D. Increasing LVAD pulsatility through changes in pump geometry. *Artif Organs* 2012;36. [Epub ahead of print] doi:10.1111/j.1525-1594.2012.01485.x
28. Magder S. The left heart can only be as good as the right heart: determinants of function and dysfunction of the right ventricle. *Crit Care Resusc* 2007;9:344–51.
29. Karantonis DM, Lovell NH, Ayre PJ, Mason DG, Cloherty SL. Classification of physiologically significant pumping states in an implantable rotary blood pump: effects of cardiac rhythm disturbances. *Artif Organs* 2007;31:476–9.
30. Karantonis DM, Cloherty SL, Mason DG, Salamonsen RF, Ayre PJ, Lovell NH. Automated non-invasive detection of pumping states in an implantable rotary blood pump. *Conf Proc IEEE Eng Med Biol Soc* 2006;1:5386–9.
31. Mason DG, Hilton AK, Salamonsen RF. Reliable suction detection for patients with rotary blood pumps. *ASAIO J* 2008;54:359–66.
32. Granegger M, Moscato F, Mahr S, Wieselthaler G, Schima HJ. Assessment of the aortic valve opening during rotary blood pump support. *ASAIO J* 2011;57:75.
33. AlOmari AH, Savkin AV, Ayre PJ, et al. Non-invasive estimation and control of inlet pressure in an implantable rotary blood pump for heart failure patients. *Physiol Meas* 2011;32:1035–60.